CHAPTER III

RESULTS AND DISCUSSION

3.1. Synthesis

Aluminum hydroxide hydrate ($Al(OH)_{3-x}H_2O$), the starting material, was calcined using the TGA to obtain the exact percentage of Al_2O_3, as indicated by the % ceramic yield. The typical Al_2O_3 content was 57.5%, as shown in Figure 3.1. This value was used throughout the experiments.

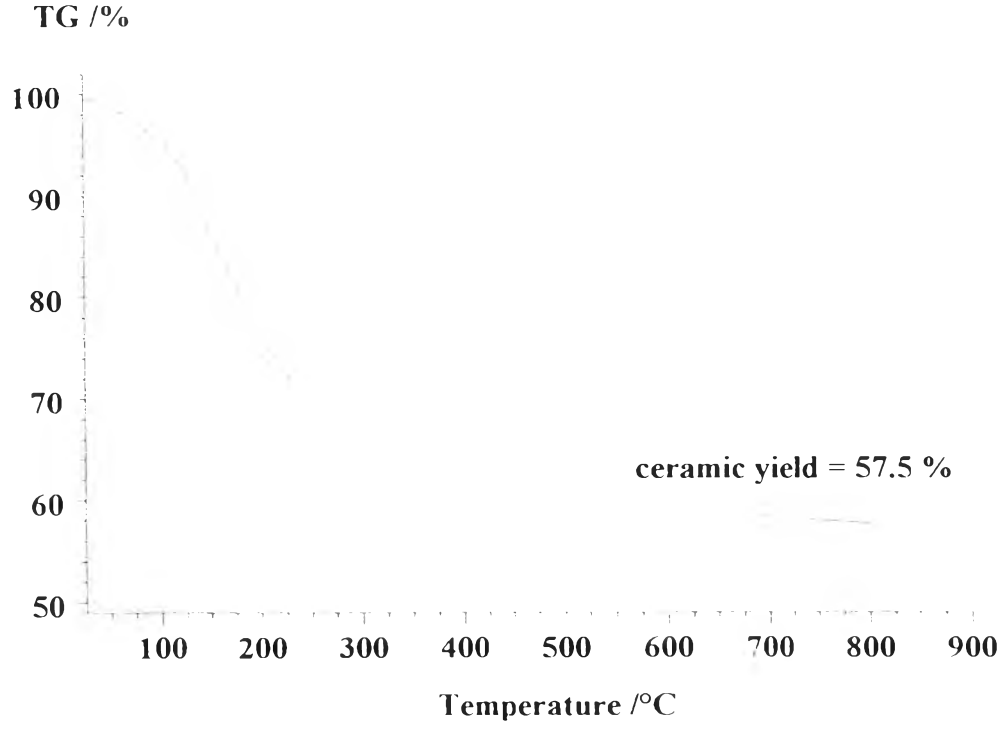

Figure 3.1 TGA Thermogram of $Al(OH)_3$.

As can be seen in Figure 3.2, with a fixed amount of aluminum hydroxide hydrate [1.77 g (22.7 mmol)] at a reaction time and temperature of 3 h. and 200 °C, respectively, the reaction went very slowly for TIS quantities less than 20 mmol. However, it went to completion when 35 mmol of TIS was used. It was found also that when 10 mmol of TETA was used with the 22.7 mmol of $Al(OH)_3$ and 35 mmol of TIS, the reaction was complete within 2 h. The yellowish product obtained from the complete reaction was soluble in methanol.

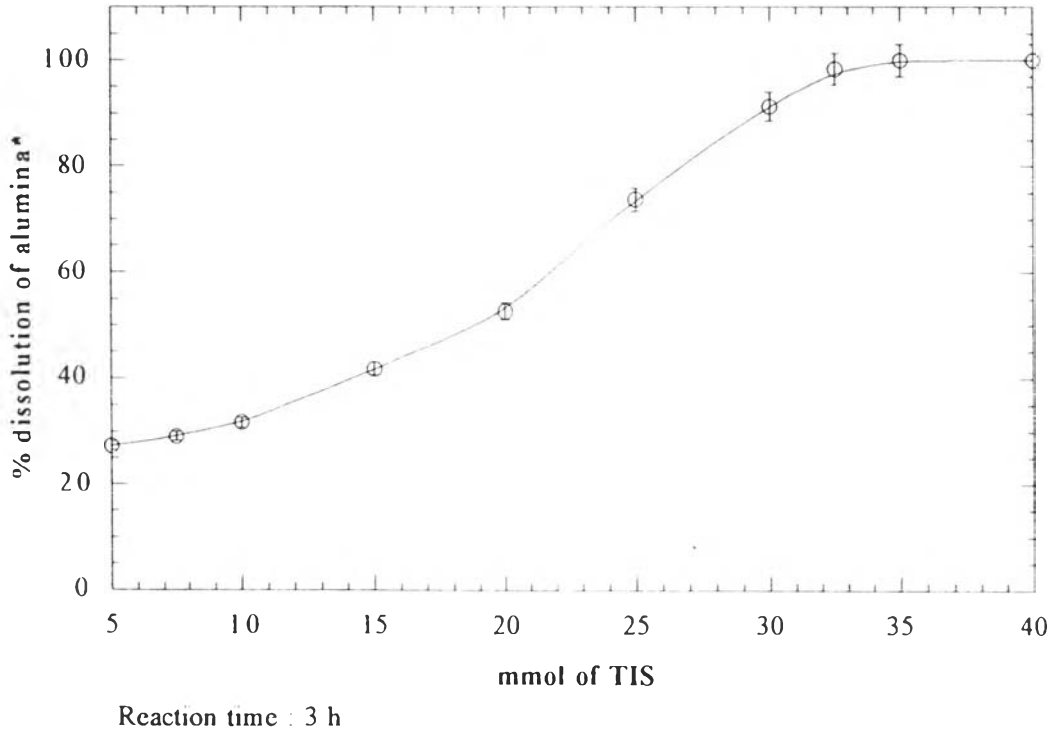

Reaction time : 3 h

Reaction temperature : 200°C

*Equivalent mmol of alumina calculated from $Al(OH)_3 \cdot xH_2O$ used

Figure 3.2 Optimization of $Al(OH)_3$:TIS Ratio for Complete Dissolution of $Al(OH)_3$.

3.2. Kinetic Studies

In this study, recovered $Al(OH)_3$ was converted to α-alumina which was then used to determine the actual amount dissolved. Aluminum hydroxide used before and after reaction was measured as alumina (Al_2O_3) using TGA ceramic yields.

3.2.1 Dissolution Rate as a Function of TIS Concentration

Concentration of aluminum hydroxide was fixed at 22.7 mmole, and the reaction time and temperature were set at 3 h, 200 °C. The amount of TIS was varied from 5, 7.5, 10, 15, to 20 mmol. The relationship between mmol alumina dissolved and mmol of TIS, see Figure 3.3, showed that when TIS concentration was less than 10 mmol, the curve was not as linear as that

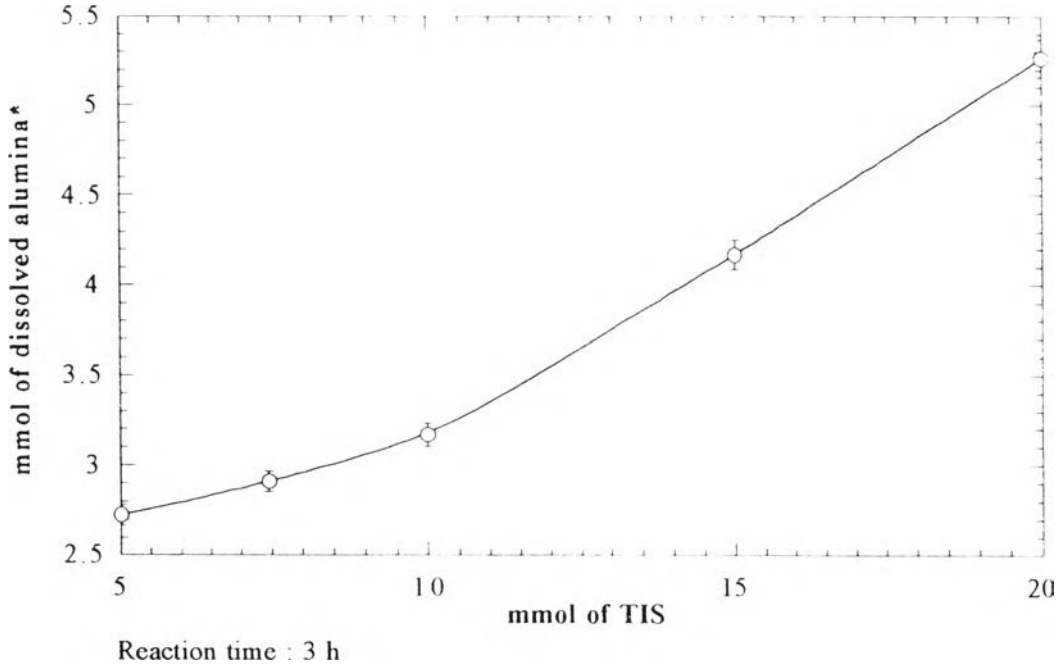

Reaction time : 3 h

Reaction temperature : 200°C

*Equivalent mmol of alumina calculated from $Al(OH)_3 \cdot xH_2O$ used

Figure 3.3 Effect of TIS Concentration.

using TIS concentration more than 10 mmol. The reason might be that there was another side reaction competing with the studying reaction. For example, the condensation of EG by TIS, as a catalyst, probably resulted in undesirable product. At very low concentration of TIS, EG was the major part of the reaction and TIS might act as catalyst to produce the product such as Al-EG [PETCHSUK et al., (1995)].

3.2.2 Dissolution Rate as a Function of $Al(OH)_3$ Concentration

The concentration of alumina was varied from 7.5 to 12.5, 15, and 40 mmol while the concentration of TIS was fixed at 20 mmol. The reaction time and temperature were set at 1 h and 200°C. The relationship between the dissolved and added alumina is nearly linear, as shown in Figure 3.4.

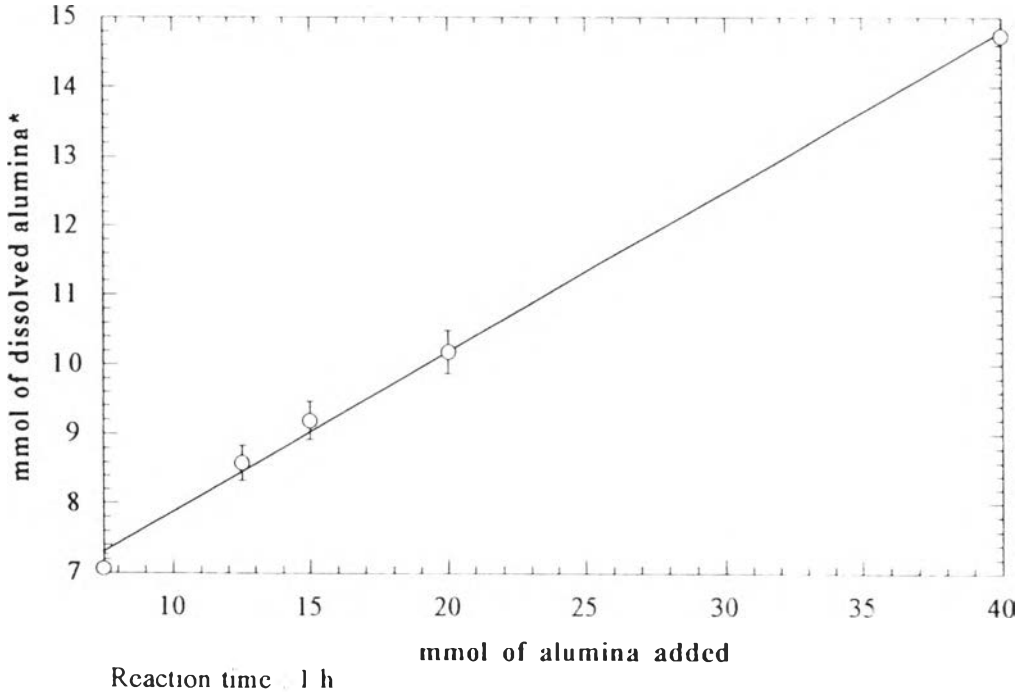

Reaction time : 1 h

Reaction temperature : 200°C

*Equivalent mmol of alumina calculated from $Al(OH)_3 \cdot xH_2O$

Figure 3.4 Dissolution Rate as a Function of $Al(OH)_3$ Concentration

Clearly, the reaction of $Al(OH)_3$ and TIS also depended on the concentration of $Al(OH)_3$. The curve was nearly linear, suggesting that the reaction was first order with respect to $Al(OH)_3$ and first order with respect to TIS. It is worth noticing that the intercept of both curves are not equal to zero. This is because some unreacted $Al(OH)_3$ was lost during recovery step.

3.2.3 Determination of the Reaction Rate Constant

In this experiment, we used the integral method to determine the reaction order. The reaction order was assumed to be second order overall, as discussed in sections 3.2.1 and 3.2.2. The amount of $Al(OH)_3$ and TIS were fixed at 22.7 mmol and 5 mmol, respectively. The reaction times were set at 15, 30, 45, 60, 75, 90, and 120 min for each temperature. The temperature was varied from 150, 170, 190, to 200°C. In this case, initial concentrations of

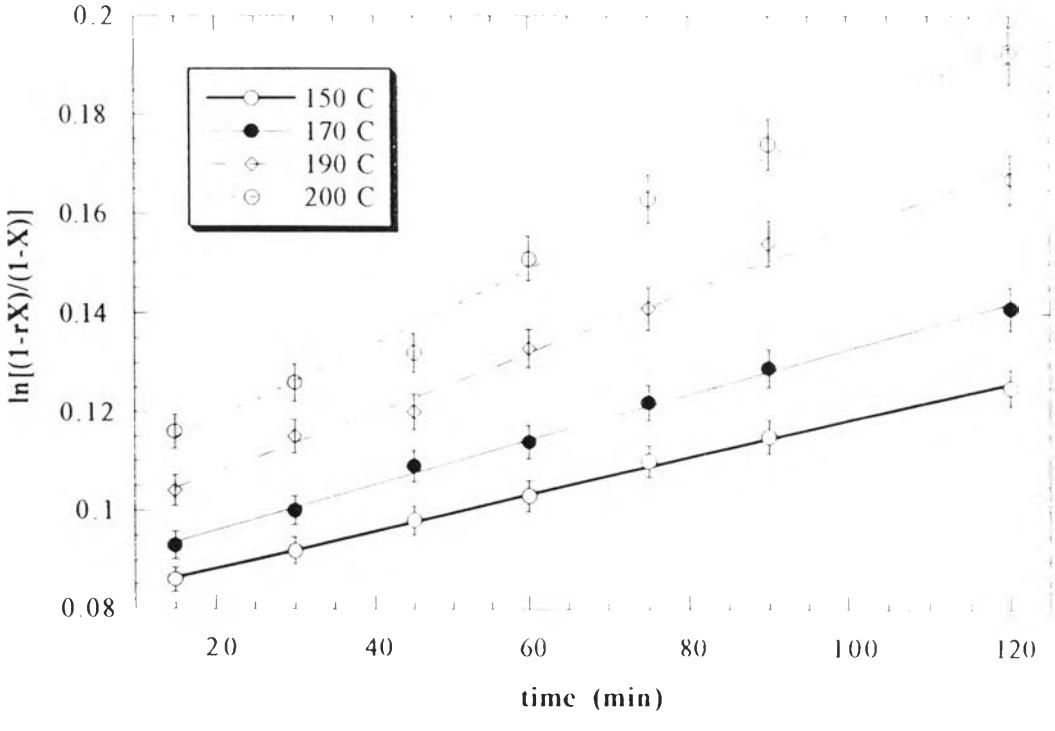

Figure 3.5 The Relationship of Logarithm of Conversion Factor versus Reaction Time for each Variation of Reaction Temperature.

both reactants were not equal Therefore, equation 1.8 was used to find the rate constant of the reaction (k) Plots of ln[(1-rX)/(1-X)] versus reaction time at each temperature are presented in Figure 3.5, (Note the linearity of the data suggesting that the reaction is most likely to be second order as assumed). The reaction rate constants were obtained from the slope of the plotted data, straight line with different gradients. As expected, the higher temperature showed the higher gradient, meaning that the higher reaction temperature, the higher dissolution rate.

3.2.4 Determination of the Activation Energy

To determine the activation energy, the Arrhenius equation was employed From section 3.2.3, after obtaining the reaction rate constants (k), ln k was plotted versus 1/T(1/Kelvin) as Figure 3.6, which gives a straight line

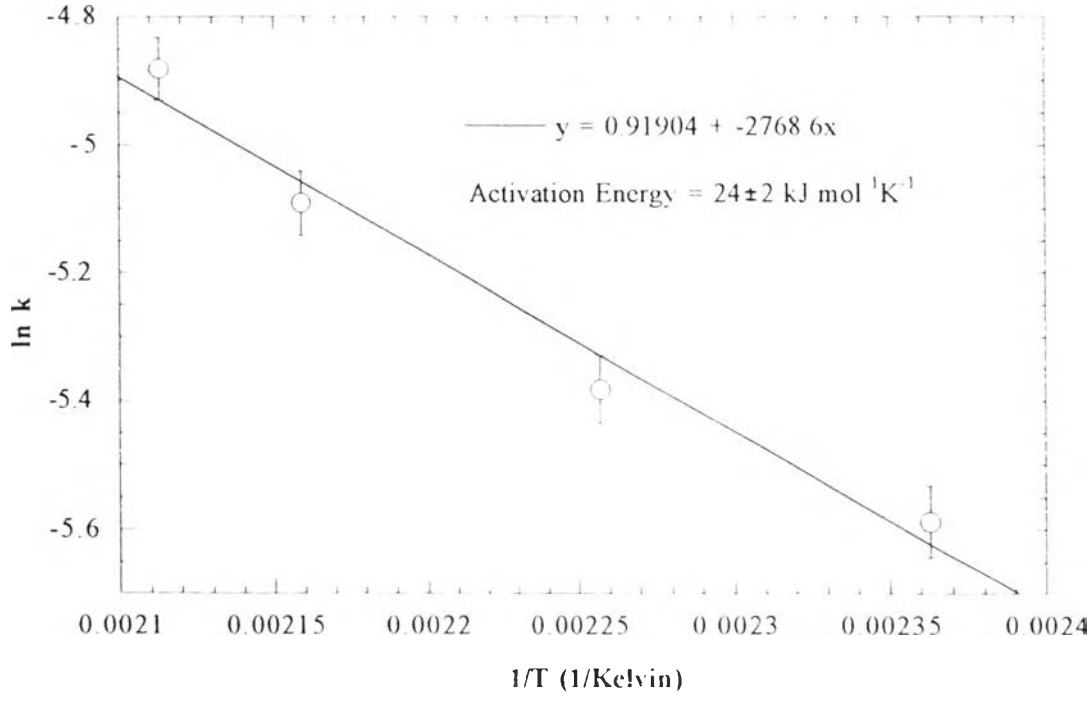

Figure 3.6 The Relationship of Logarithm of Rate Constant and Reaction Temperature.

with the slope proportional to the activation energy The slope obtained is equal to the activation energy devided by the gas constant (8.314 J mol^{-1} K^{-1}). As a result, the activation energy was 24±2 KJ mol^{-1}

3.2.5 Dissolution Rate as a Function of TETA Concentration

The plot of the amount of dissoved $Al(OH)_3$ and amount of TETA is presented in Figure 3.7. The higher the TETA concentration, the greater the amount of dissolved $Al(OH)_3$ At low TETA concentration (1.25-2.5 mmol), the amount of $Al(OH)_3$ dissolved increased significantly, as compared to the higher TETA concentrations.

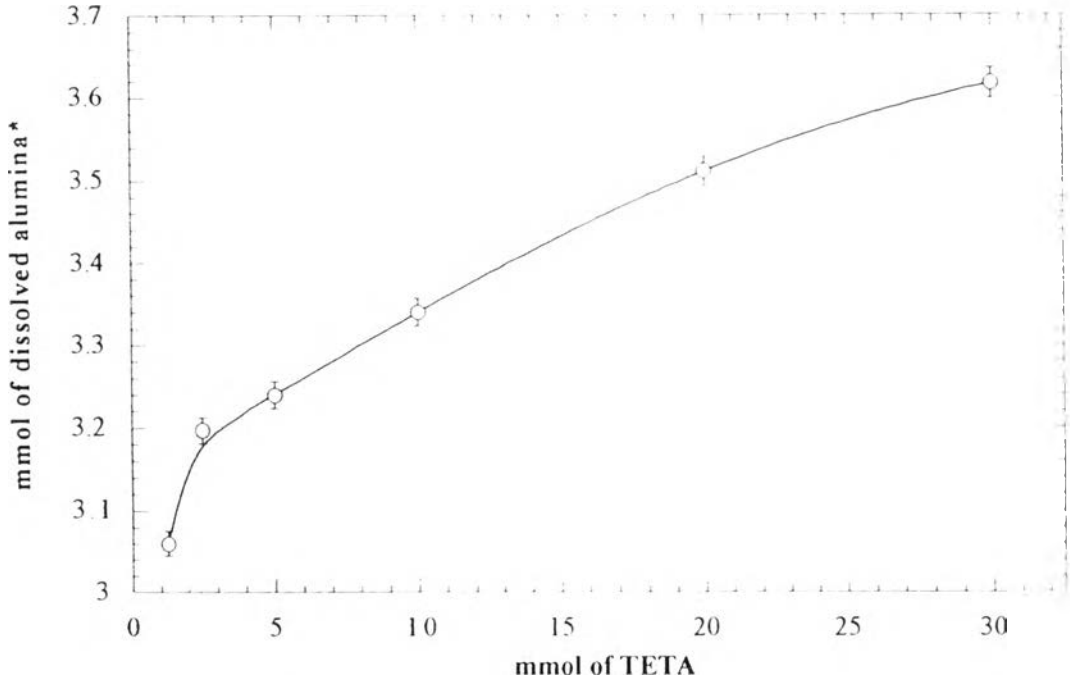

*Equivalent mmol of alumina calculated from $Al(OH)_3$ xH_2O used

Figure 3.7 Effect of the TETA Concentration

3.2.6 Dissolution Rate as a Function of Time in the Presence of TETA, as a Catalyst

Figure 3.8 shows a plot of mmol of unreacted $Al(OH)_3$ versus reaction time comparing reactions with (1.25 mmol) and without TETA. The dissolution reaction rate with TETA was faster than that without TETA because TETA increased solubility of $Al(OH)_3$ which caused the reaction to go faster.

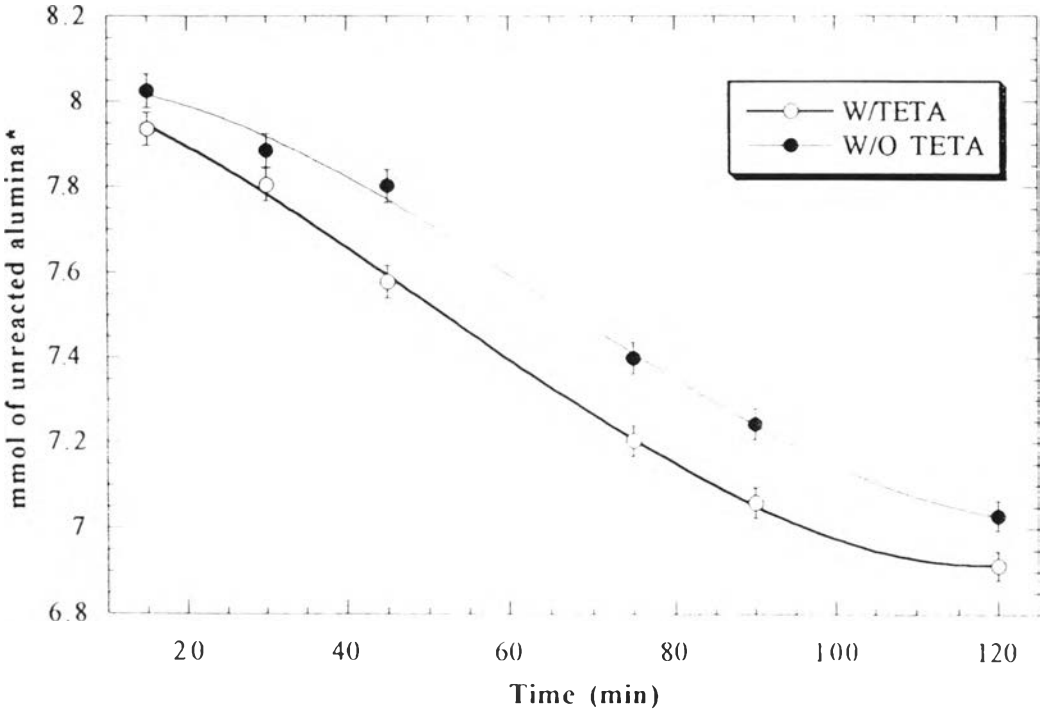

*Equivalent mmol of alumina calculated from $Al(OH)_3 \cdot xH_2O$ used

Figure 3.8 Effect of TETA Concentration with Time.

3.3 Characterization

3.3.1 Thermogravimetric Analysis

The TGA data for the product from the reaction without TETA (Figure 3.9) shows two major regions of mass loss. The first region was between 180°-260°C that indicated the decomposition of TIS which is a component of the product while the second region occurred at about 260°-550°C which corresponded to the oxidative decomposition of the organic ligands and carbon residues. The % ceramic yield of the product was 27.6 %, which was higher than the theoretical ceramic yield (23.7 %). The higher % ceramic yield might result from the presence of smaller units of oligomers in the product, as indicated by FAB$^+$-MS

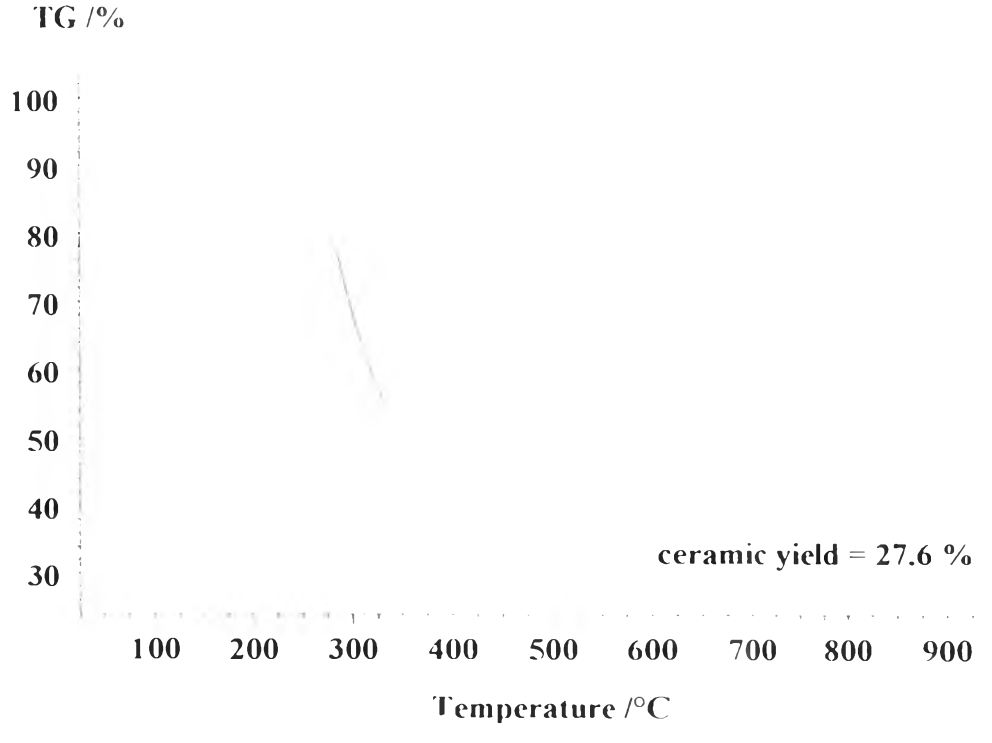

Figure 3.9 TGA Thermogram of the Product from the Reaction without TETA.

The TGA of the product synthesized in the presence of TETA (Figure 3.10), also showed two major mass losses at 180°-250°C and 250°-500°C that corresponded to the decomposition of TIS and the oxidative decomposition of the organic ligands, and carbon residues, respectively. The % ceramic yield of product was 31.9 %, which was much higher than the theoretical yield. This can be explained along with the mass spectrum which indicated that the product synthesized from the batch with TETA gave more dimer (m/e 431) than the one without TETA because mass spectral data showed that the product consists of monomer, trimer, pentamer, and hexamer. The more smalller unit, the higher ceramic yield. This is why the product from the reaction with TETA gives higher ceramic yield than the one without TETA.

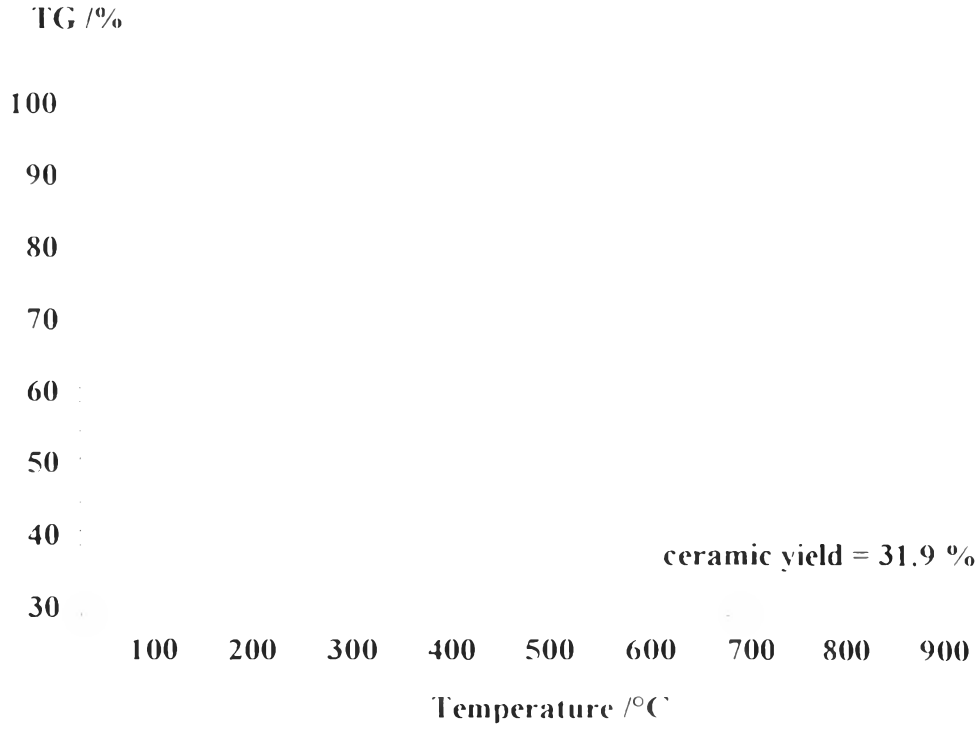

Figure 3.10 TGA Thermogram of the Product from the Reacton with TETA

3.3.2 *Differential Scanning Calorimetry*

The DSC of the product from the reaction without TETA (Figure 3.11) showed an exotherm at 250°-280°C corresponding to the boiling point of TIS, since when the product was run the second time, there was no exothermic peak in DSC thermogram. An endotherm at 380°-400°C, as compared to its TGA, correlated to the decomposition temperature of products. The T_g was observed at about 167°C.

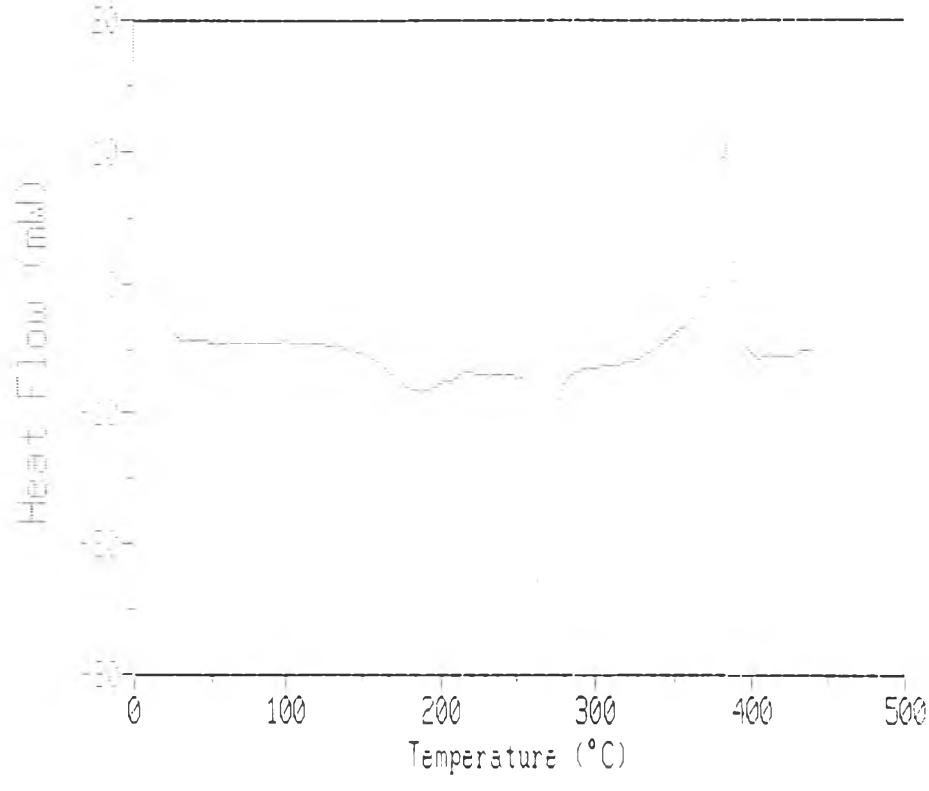

Figure 3.11 DSC Thermogram of the Product from the Reacton without TETA.

Similarly, the DSC data of the product from the reaction with TETA (Figure 3.12) showed the exotherm at about 220°-260°C corresponding to the decomposition of TIS. An endotherm at about 350°-400°C was again the decomposition temperature of products. The T_g of this product occured at about 166°C

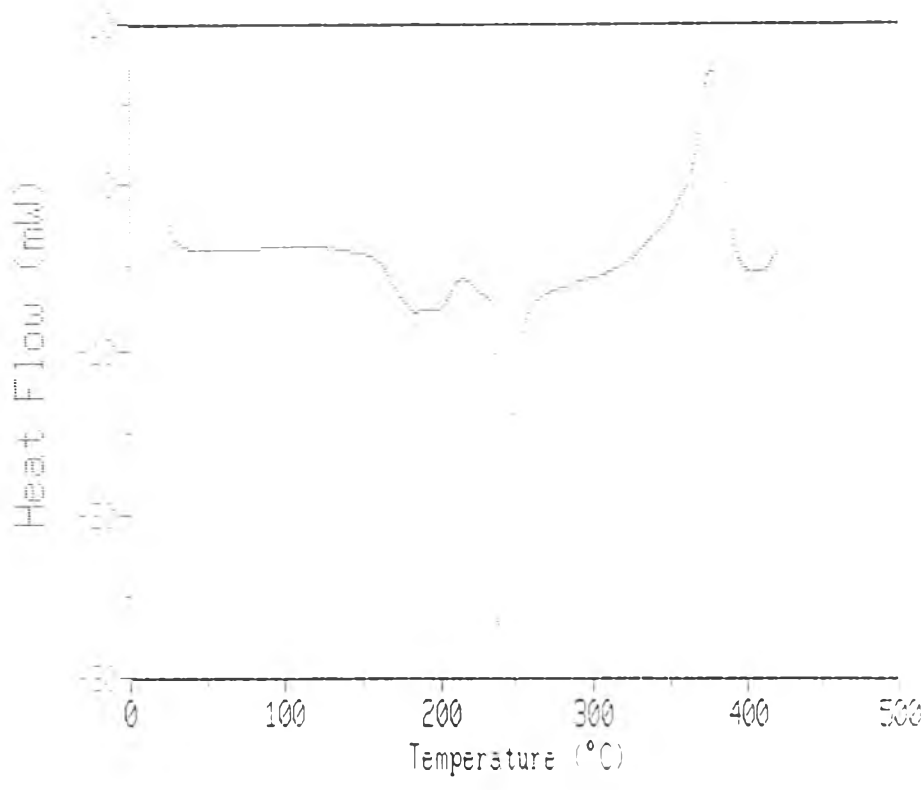

Figure 3.12 DSC Thermogram of the Product from the Reaction with TETA.

3.3.3 FAB -Mass Spectroscopy

Mass spectral analysis suggests that there are four different alumatrane complexes; hexamer (m/e 1292), the highest intensity pentamer plus one morpholine (m/e 1250), trimer plus one ethylene glycol (m/e 707), and monomer plus one TIS (m/e 409) and the intensities of all proposed structures was shown in table 3.1.

Table 3.1 The Proposed Structures and Fragmentation Pattern of Products

m/e	Intensities	Proposed Structure
216	50	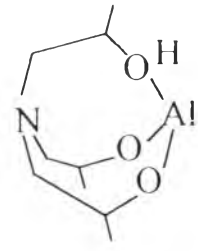 $AlN(CH_2CH_2CH_3O)_3H^+$
409	17.5	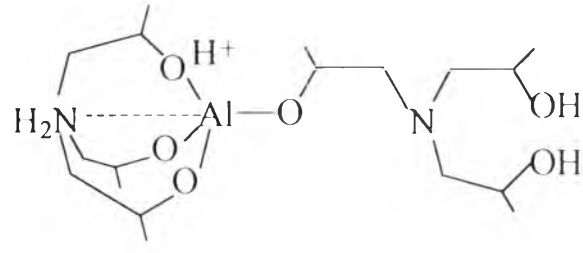 $AlN(CH_2CH_2CH_3O)_3N(CH_2CH_2CH_3O)(CH_2CH_2CH_3OH)_2H^+$
492	38.7	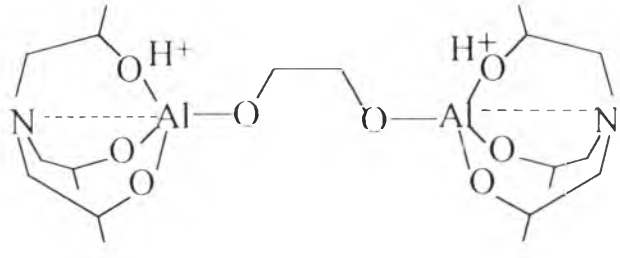 $Al_2[N(CH_2CH_2CH_3O)_3]_2(OCH_2CH_2O)H_2^+$
707	35.4	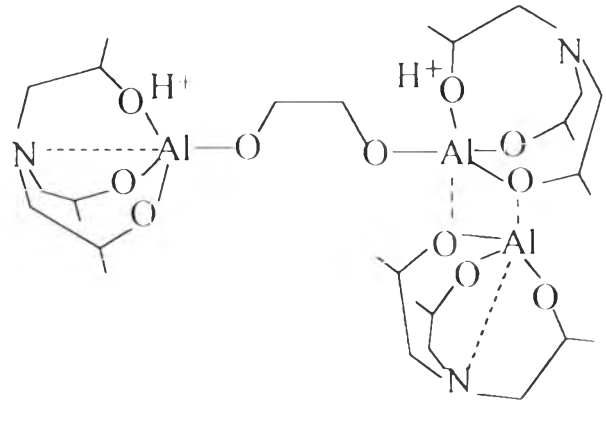 $Al_3[N(CH_2CH_2CH_3O)_3]_2(OCH_2)_2H_2^+$

m/e	Intensities	Proposed Structure
959	7.9	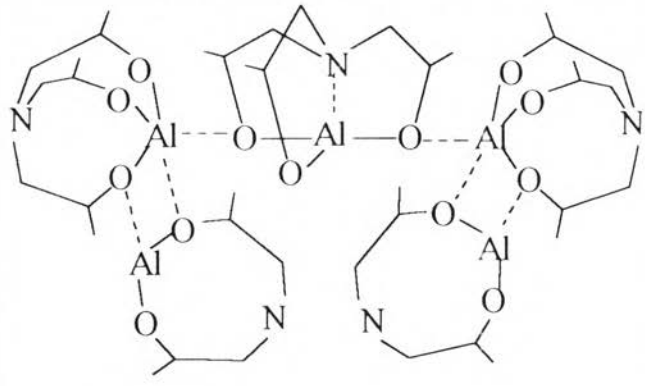 $Al_3[N(CH_2CH_2CH_3O)_3]_2Al_2[N(CH_2CH_2CH_3O)_2]_2$
1076	15	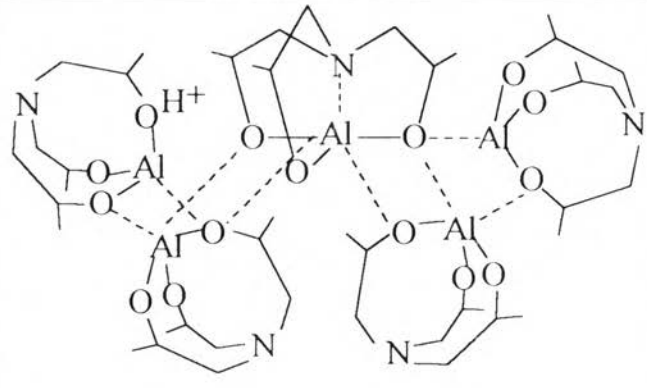 $Al_5[N(CH_2CH_2CH_3O)_3]_5H^+$
1175	46.3	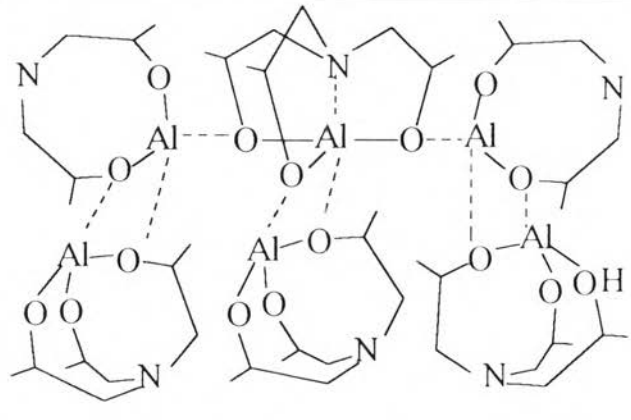 $Al_4(CH_2CH_2CH_3O)_3]_4Al_2[N(CH_2CH_2CH_3O)_2]_2H^+$

m/e	Intensities	Prosposed Structure
1250	100	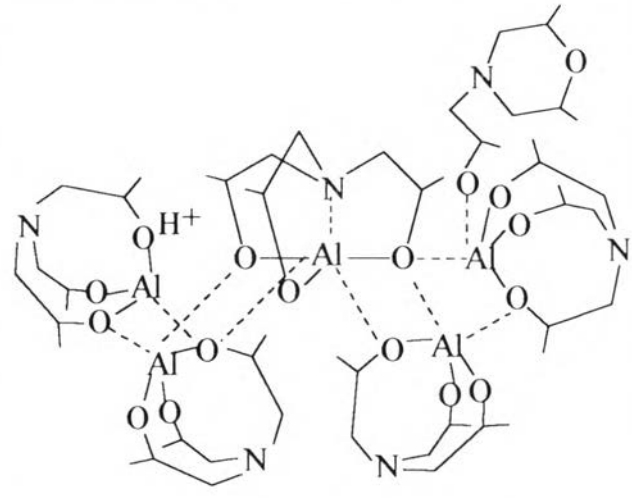 $Al_5[N(CH_2CH_2CH_3O)_3]_5N(CH_2CH_2CH_3O)_2CH_2CH_2CH_3H^+$
1292	7.8	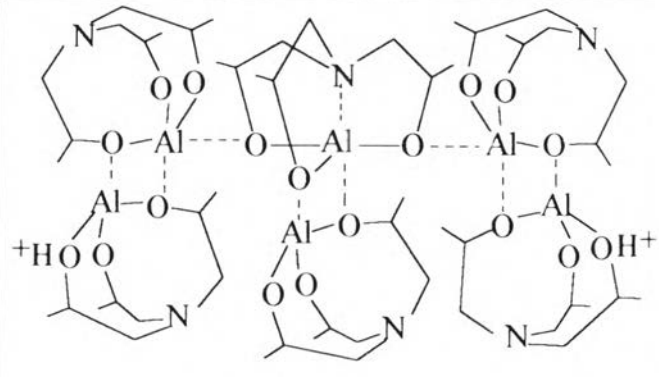 $Al_6[N(CH_2CH_2CH_3O)_3]_6H^+$

Fragmentation patterns of these complexes would be as follow;

$$\text{m/e} \quad 1292 \xrightarrow{-2(CH_2CHCH_3O)} 1175$$

$$\text{m/e} \quad 1250 \xrightarrow{-N(CH_2CHCH_3)_2O} 1076 \xrightarrow{-2(CH_2CHCH_3O)} 959$$

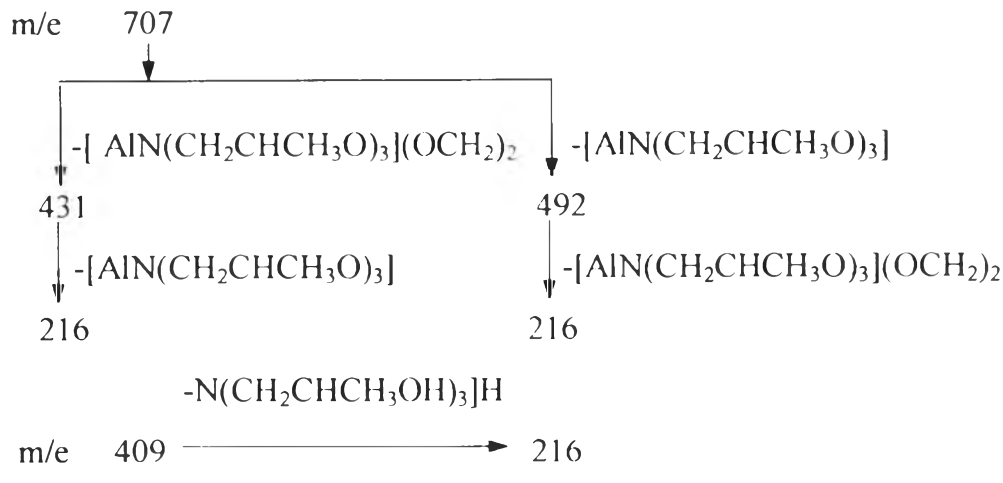

The fragmentation pattern of the product from the reaction with TETA was similar to that without TETA. However, the intensity of the base peak at m/e 1250 for the product without TETA was higher than the product with TETA whereas the intensity of the peak at m/e 216 was lower. Again, TETA accelerates the reaction to completion faster and gives the smaller unit of oligomer (m/e 409). The most stable species of both reactions showed highest intensity peak at m/e 1250, as structured in Table 3.1.

3.3.4 Nuclear Magnetic Resonance Spectroscopy

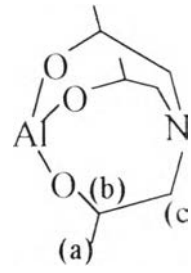

The ^{1}H-NMR spectrum of the product from the reaction without TETA showed 3 multiple peaks. The peaks at 1.07-1.41 ppm correspond to the -CH_3 group of TIS (position (a)). The peaks at 2.36-3.15 ppm are assigned to the methylene group adjacent to the N-atom of TIS (-N-CH_2) at position (c). The peaks at 3.65-4.23 ppm are assigned to the tertiary carbon adjacent to the O-atom of TIS, position (b). The ^{1}H-NMR spectrum of the product from the reaction with TETA gave a similar spectrum

The ^{13}C-NMR spectrum of the product from the reaction without TETA showed a multiple peak at 21.59-22.45 ppm corresponding to -CH_3 groups at position (a) coupled to itself and proton of the tertiary carbon. The sharp peak at 64.30 ppm belongs to the carbon adjacent to N-atom of TIS (-N-CH_2) at position (c). The multiple peak at 78.97-79.48 ppm is associated with the carbon adjacent to O-atom of TIS (position (b)) due to the coupling with -N-$\underline{CH_2}$ and -$\underline{CH_3}$. The spectrum of both reactions showed the similar positions. Another reason for having multiple peaks at 3 positions is that the products contain several kinds of oligomers, such as monomer, dimer, etc.

The ^{27}Al-NMR spectra of the products from the reaction with and without TETA showed 3 multiple peaks, as shown in Table 3.2.

Table 3.2 Peak Positions of ^{1}H- , ^{13}C-, and ^{27}Al-NMR of Products

Compounds	^{1}H-NMR (ppm)	^{13}C-NMR (ppm)	^{27}Al-NMR (ppm)
Product w/o TETA	1.07-1.41 (a) 2.36-3.15 (c) 3.65-4.23 (b)	21.59-22.45 (a) 64.30 (c) 78.56-79.21	7.5 49.6 66.0
Product w/ TETA	1.07-1.88 (a) 2.23-2.85 (c) 3.73-4.11 (b)	20.79 (a) 64.30-65.63 (c) 78.79-79.48 (b)	7.4 48.8 64.9

3.3.5 Fourier Transform Infrared Spectroscopy

Figure 3.11 shows the FTIR spectra of the products from the reactions with and without TETA. Both spectra show similar functional groups. The peaks at 3000-3700 cm^{-1} correspond to ν O-H and ν C-H. The singlet peak at about 1650 cm^{-1} is O-H overtone and C-H bending. The strong peak at 1000-1250 cm^{-1} results from the ν C-N and/or O-H bending. The broad peak at 500-800 cm^{-1} represents the ν Al-O of the product.

Table 3.3 Peak Position and Assignments of FTIR Spectra of Products with/without TETA

peak positions		assignments
Al-TIS	TIS-Al-TETA	
3000-3700	3000-3700	u O-H and u C-H
2750-3000	2750-3000	u C-H
1650	1630	O-H overtone; C-H bending
1450	1450	δ C-H
1000-1200	1000-1250	u C-N; O-H bending
500-800	500-800	u Al-O

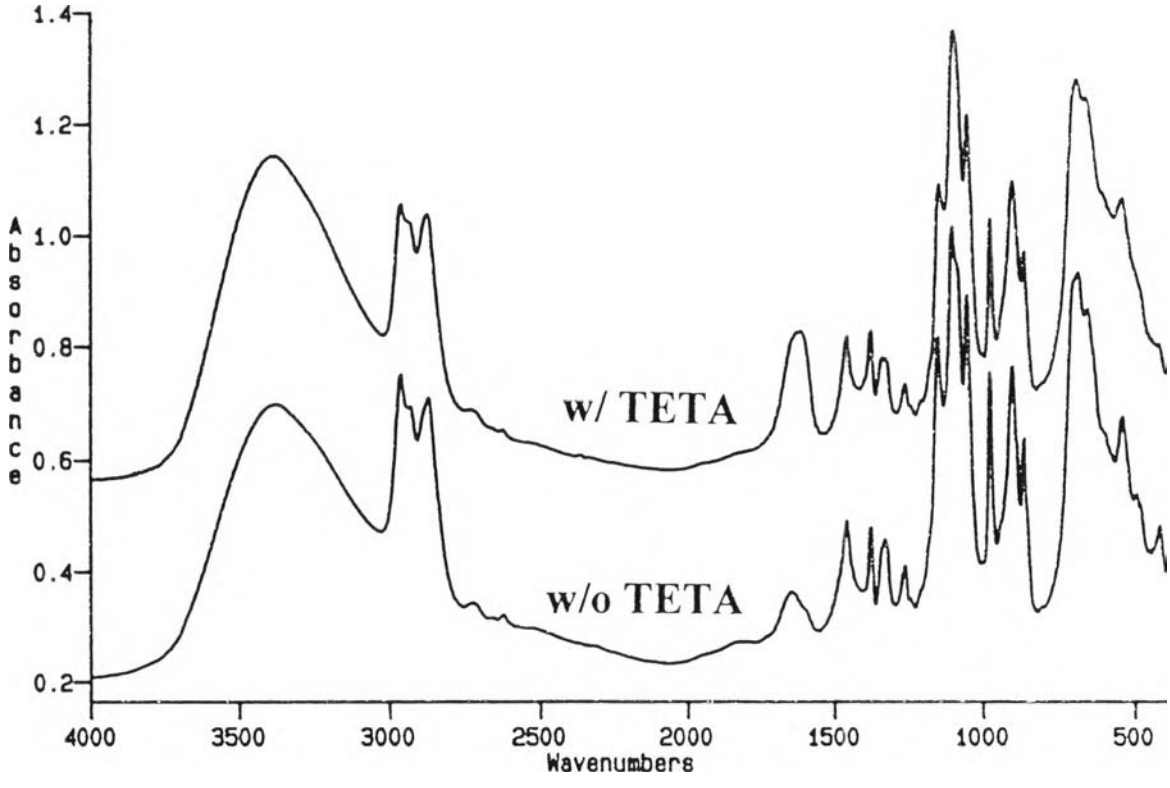

Figure 3.13 FTIR Spectra of the Products from the Reaction with/without TETA.